Energy 342 (2026) 139715

Contents lists available at ScienceDirect

Energy

journal homepage: www.elsevier.com/locate/energy

Dynamic simulation of a liquefied hydrogen export terminal

Federica Restelli [a], Fuyu Jiao [b], Bruce Norris [b,c], J.P. Martin Trusler [d], Arman Siahvashi [e], Eric F. May [b,c], Laura A. Pellegrini [a], Michael Johns [b,c], Saif Z.S. Al Ghafri [b,c,f,*]

[a] *GASP–Group on Advanced Separation Processes & GAS Processing, Dipartimento di Chimica, Materiali e Ingegneria Chimica "G. Natta", Politecnico di Milano, Piazza Leonardo da Vinci 32, 20133, Milano, Italy*
[b] *Fluid Science and Resources Division, Department of Chemical Engineering, Faculty of Engineering and Mathematical Sciences, The University of Western Australia, Crawley, WA, 6009, Australia*
[c] *Future Energy Exports Cooperative Research Centre, 35 Stirling Hwy, Crawley, WA, 6009, Australia*
[d] *Department of Chemical Engineering, Imperial College London, London, SW7 2AZ, United Kingdom*
[e] *Faculty of Engineering, School of Aerospace, Mechanical, and Mechatronic Engineering, The University of Sydney, Australia*
[f] *Centre for Hydrogen and Renewable Energy (CHRE), CQUniversity, Gladstone Marina Campus, 43 Bryan Jordan Drive, Callemondah, Qld, 4680, Australia*

ARTICLE INFO

Keywords:
Liquid hydrogen
Boil-off gas
Carrier loading
Liquid hydrogen storage
Liquid hydrogen transport
Hydrogen export

ABSTRACT

At prospective liquid hydrogen (LH_2) export terminals, managing boil-off gas (BOG) presents a significant challenge that has not been adequately explored in the literature. This work is a case study examining the management of BOG evolved during storage and carrier loading at an export terminal, carried out using detailed dynamic simulations. The considered terminal operates with a LH_2 production rate of 450 t/d, and a carrier capacity of 160000 m^3. The normal operation cycle spans a period of 28 days, during which all the generated BOG is recovered. The estimated levelized cost for terminal storage and shipment is 2.77 USD/kg, underlining the need for further research to reduce costs and enhance the economic viability of LH_2 export. A sensitivity analysis indicates that the production rate primarily affects the duration of the normal operation cycle and, consequently, shipping frequency, while feed pressure and ortho-para hydrogen composition significantly influence total BOG generation.

Abbreviations:

BOG	Boil-Off Gas
CAPEX	Capital Expenditure
CEPCI	Chemical Engineering Plant Cost Index
DNV	Det Norske Veritas
HESC	Hydrogen Energy Supply Chain
ID	Inner Diameter
IEA	International Energy Agency
IRAS	Integrated Refrigeration And Storage
KHI	Kawasaki Heavy Industries
LCOH	Levelized Cost Of Hydrogen
LH_2	Liquid Hydrogen
LNG	Liquefied Natural Gas
MLI	Multi-Layer Insulation
OD	Outer Diameter
OPEX	Operating Expenditure
PFD	Process Flow Diagram
PV	Process Variable
SP	Set Point
VIP	Vacuum Insulated Pipeline

1. Introduction

According to the International Energy Agency (IEA), global demand for hydrogen was 94 Mt/y in 2021. The IEA projects that demand could grow to 150 Mt by 2030 and 600–650 Mt/y by 2050 [1]. Forty-one countries worldwide have now adopted hydrogen strategies to increase and facilitate the production and use of hydrogen as a fuel [2]. For example, the United States Department of Energy has a roadmap outlining opportunities for a clean hydrogen supply that could reach 50 Mt/y by 2050 [3]. Meanwhile, Australia aims to position itself as a global leader in hydrogen exports and decarbonizing local industries by the end of this decade [4]. As both supply and demand continue to grow, developing related storage technologies and improving the associated infrastructure will become increasingly important. Due to its low density

* Corresponding author. Centre for Hydrogen and Renewable Energy (CHRE), CQUniversity, Gladstone Marina Campus, 43 Bryan Jordan Drive, Callemondah, Qld, 4680, Australia

E-mail address: s.alghafri@cqu.edu.au (S.Z.S. Al Ghafri).

https://doi.org/10.1016/j.energy.2025.139715
Received 17 January 2025; Received in revised form 2 November 2025; Accepted 16 December 2025
Available online 17 December 2025

at standard conditions (0.09 kg/m^3), hydrogen must be compressed or liquefied to enable its efficient storage and transportation. Alternatively, it can be converted into other compounds that act as carriers, such as ammonia [5], methanol [6], or methylcyclohexane [7]. When considering large-scale hydrogen transportation, liquefied hydrogen appears to be one prospective option, as: i) its mass density is about 800 times greater than that of gaseous hydrogen at standard conditions; ii) it does not require further energy for dehydrogenation or release greenhouse gases and other pollutants (CO_2, NO_x and N_2O) compared to methanol and ammonia [8]. To realise this potential, it will be essential to address the challenges presented by its cryogenic nature and reduce the associated costs of liquefaction, storage and transportation [8].

In Australia alone, several international liquid hydrogen (LH_2) transportation projects are actively being considered. In 2022, the Hydrogen Energy Supply Chain (HESC) pilot project made history by successfully exporting LH_2 from the Port of Hastings (Victoria, Australia) to Kobe (Japan). This milestone proved the feasibility of exporting LH_2 and laid the groundwork for the project partners to develop a larger-scale liquefied hydrogen supply chain commercial project between Victoria and Japan. The main facilities involved in this prospective larger-scale export project include two 60 t/d hydrogen liquefiers, five 10000 m^3 storage tanks at the export terminal, a 160000 m^3 ship comprising four tanks (only one of which will be used during the initial phase), and a 50000 m^3 storage tank at the import terminal [9]. LATTICE Technology and LH2 Energy are advancing a liquefied hydrogen export chain from Darwin (Northern Territory, Australia) to Korea. They are currently conducting the basic design for a 75000 m^3 liquefied hydrogen export and import terminals [10]. Another project based in Darwin is the Darwin Green Liquid Hydrogen export project, which aims to demonstrate large-scale LH_2 export at a rate of 21000 t/y to the Japanese transport sector by 2030. Future expansion of this project is planned, potentially increasing total LH_2 capacity to 126000 t/y [11]. The Central Queensland Hydrogen (CQ-H2) project is currently studying the development of a large-scale renewable hydrogen production facility near Gladstone and a liquefaction plant at the Port of Gladstone. The project focuses on exporting LH_2 to Japan and supplying hydrogen for ammonia production for both domestic and export markets. It involves a phased development approach, initially aiming to produce approximately 200 t/d of green hydrogen by 2029, with plans to scale up to 800 t/d by the early 2030s [12].

At prospective LH_2 export terminals, one of the main challenges to be addressed is the boil-off gas (BOG) generation and management. Boil-off gas refers to the vapour generated when LH_2 boils due to heat ingress and changes in operating conditions. Several factors contribute to BOG generation at the export terminal: (1) flashing due to depressurization of LH_2, (2) heat added by equipment such as pumps, (3) vapour displacement, (4) heat input from the environment, (5) heat absorbed following contact with warmer equipment (e.g. during LH_2 loading), and (6) incomplete ortho-para hydrogen conversion at the outlet of the liquefaction plant. This dynamic BOG generation can significantly impact system performance and pose serious safety risks. Efficient management of generated BOG is therefore crucial for economic and safety reasons and involves land-based storage tanks and maritime vessels.

Kim et al. [13] have reviewed the technical aspects and challenges to be addressed when developing a liquefied hydrogen export terminal, including BOG. Morales-Ospino et al. [14] reviewed various strategies to minimize hydrogen evaporation and recover BOG, including zero boil-off, hydrogen reliquefaction, and commercial solutions for boil-off hydrogen compression. Gursu et al. [15] optimised liquid hydrogen boil-off losses by analysing ortho-para conversion and heat leakage through mechanical supports. They evaluated optimal ortho-hydrogen concentrations for different storage scenarios, ideal placement of cooling stations, and optimal storage pressures to minimize energy losses and improve storage efficiency. Okpeke et al. [16] used an analytical approach to investigate the reduction of boil-off losses during the initial filling of LH_2 in an empty cryogenic tank by precooling the tank with liquid nitrogen or helium to reduce thermal gradients between the liquid hydrogen and the tank surface. Wang et al. [17] modelled the impact of allowing LH_2 tanks to self-pressurise during maritime transport to reduce boil-off losses. Results showed that modest increases in tank pressure can significantly cut losses (up to 91 % at 60 kPag) highlighting self-pressurisation as an effective strategy for low-loss LH_2 storage over short voyages. Smith et al. [18] introduced a modelling approach to estimate fuel boil-off in LH_2 carriers, accounting for tank design, weather conditions, and ship speed. They showed that a LH_2 carrier with the same tank volume and glass wool insulation thickness as a conventional liquefied natural gas (LNG) carrier stores only 40 % of the fuel energy and exhibits a boil-off rate 9 times higher, with double the sensitivity to sloshing. Kim et al. [19] proposed a BOG handling system that produces fuel for a LH_2 carrier and liquefies excess BOG using a Claude cycle. Similarly, Choi et al. [20] studied boil-off gas management for LH_2 carriers, suggesting partial reliquefaction with a reverse Brayton cycle while using the non-liquefied hydrogen fraction in a fuel cell to generate electricity. Ravichandran and Cavaliere [21] analysed seasonal variations in liquid hydrogen boil-off rates in a stationary small-scale tank (5.6 m^3 capacity) using temperature data and dynamic simulations. Results showed significant boil-off rate fluctuations across seasons, highlighting the need for effective thermal management systems to minimize hydrogen losses. Petipas [22] investigated the dynamic behaviour of BOG losses during transfer at a LH_2 refuelling station.

To the authors' knowledge, the dynamic behaviour of BOG generation during LH_2 storage at harbour facilities and during carrier loading operations has not yet been detailed in the open literature, despite the growing interest in the liquid hydrogen supply chain. This gap in critical data concerning the characterisation and control of BOG during both storage and loading processes limits the development of standardised management and operational practices. Knowing the rate of BOG generation as a function of time and understanding the impact and management of boil-off gas on liquid hydrogen plant configurations from stationary storage to ship loading is essential for ensuring both safety and operational efficiency. To address this knowledge gap, this study delivers a novel and in-depth analysis that extends beyond the current body of literature, offering practical strategies for the effective control and management of BOG. Specifically, in response to the industrial need for designing LH_2 export terminals capable of mitigating BOG generation and preventing product losses, economic penalties, and safety risks, the objective of this work is to study the evolution of BOG during storage and carrier loading operations at an export terminal using detailed dynamic simulations. The considered case study is characterised by a liquid hydrogen production rate of 450 t/d and a carrier capacity of 160000 m^3. The base value of 450 t/d is chosen as an exemplar as it equates approximately to the current global liquid hydrogen market [8], which is predominately used for space applications and in the semiconductor sector. While the storage and transport of hydrogen in its liquid form is currently small, this is expected to grow significantly [8]. Detailed sensitivity analysis is conducted to ensure main finding from this case study is applicable to other cases including different storage and shipment capacities.

In Section 2, a review of state-of-art technologies is provided. Section 3 describes the system as studied in this work. Section 4 details the dynamic simulation method and the scenarios investigated. The results, including economic assessments and sensitivity analyses on the design and operating parameters, are presented and discussed in Section 5.

2. State-of-the-art technologies

2.1. LH_2 storage tanks

There are only a few large-scale LH_2 storage tanks worldwide. Among them is NASA's 4700 m^3 spherical tank, which began construction in 2019 to support the Space Launch System heavy-lift rocket for the Artemis program. The inner vessel of this tank is made of Grade

304 stainless steel, while the outer shell is made of carbon steel [23]. The tank incorporates two energy-saving technologies: a glass-bubble filled vacuum insulation system and an Integrated Refrigeration And Storage (IRAS) heat exchanger. The IRAS features a heat exchanger system within the internal container that removes heat from the bulk liquid hydrogen using an external helium cryocooler, thereby achieving zero boil-off. Another large-scale LH_2 storage tank was built in Japan in 2020, with a storage capacity of 2250 m^3. It was part of the world's first LH_2 terminal in Kobe (Japan), built to receive LH_2 transported from Australia. This tank also features a double-walled vacuum-insulated construction with the vacuum space filled with perlite powder [24], which, like the glass bubbles in NASA's tank, serve to reduce radiative heat leak into the storage tank. In the same year, Kawasaki Heavy Industries announced the basic design for a 11200 m^3 spherical tank with an operating capacity of 10000 m^3 and a boil-off rate of less than 0.1 % per day [25]. In 2023, Samsung C&T Engineering & Construction Group received certification from the internationally accredited certification body Det Norske Veritas (DNV) for a method to construct a cryogenic storage tank with a capacity of 40000 m^3 [26]. Samsung C&T is working with Whessoe, a global leader in designing and manufacturing low-temperature and cryogenic storage tanks, to refine the technology for this DNV-certified project [27].

Following the standard practice of the LNG industry, tank cool-down may be achieved by spraying LH_2 from the top, with a typical cool-down rate of less than 40 K/h. Cool-down rates are influenced by the properties of the tank material (resistance to thermal stresses, thermal conductivity) and the pressure build-up rate within the tank due to the boil-off. Strong temperature gradients, particularly if non-linear, result in stresses which may lead to rupture. In LNG operations, during tank filling, liquid from the bottom of the tank must be pumped and sprayed onto the upper part to minimize temperature gradient and mitigate thermal stratification and prevent rollover with subsequent rapid BOG generations. According to LNG practice, a typical storage tank has maximum and minimum design pressures of 2.0 psig (0.138 barg) and 0 psig (0 barg), respectively. Gauge pressure control is often used, with the normal operating pressure of the tank being 0.9 psig (0.062 barg) [28].

2.2. LH_2 pumps and BOG compressors

LH_2 loading pumps are of the submersible type and are located within the storage tanks. Submersible pumps are commonly utilized to prevent the risk of leakage owing to the higher hydrostatic pressure at the bottom of storage tanks, where the pipeline connection points are located. The design features a sealed motor, forming a single unit submerged in LH_2. The heat dissipated and electrical dissipation is directly transferred to the stored LH_2. The relatively low density of LH_2 can lead to a low available net positive suction head, resulting in only a small difference between the saturated vapour and liquid pressure. Consequently, an adequate liquid head over the pump must always be maintained during pumping to prevent cavitation. Commercially available submersible LH_2 pumps include those manufactured by Cryostar and Nikkiso. Cryostar offers submersible LH_2 pumps with a capacity of up to 500 m^3/h [29].

Boil-off gas compressors are needed to maintain storage tank pressure within their operating ranges and recycle BOG to the liquefaction plant or other applications. They do not require a large compression ratio, but compressing BOG at cryogenic temperatures is a significant engineering challenge. Only a few companies, including Atlas Copco and Air Products, claim to supply compressors that operate at such low suction temperatures. However, these have not been demonstrated commercially, and factors such as material embrittlement and gas seal reliability at such cryogenic temperatures need to be evaluated. An alternative is to preheat the BOG and use commercially available reciprocating compressors, which require the hydrogen to be around ambient temperature.

2.3. LH_2 pipelines and loading arms

Pipelines used for circulation and loading are the largest sources of heat input into the fluid due to their high surface area to volume ratio and long lengths. Liquid hydrogen is circulated or loaded at elevated pressure to avoid boil off and phase separation within the pipelines. However, the BOG due to heat input increases during the pressure reduction to storage conditions. The pipeline diameter is generally determined by considering the maximum pressure drop per unit length, which depends on fluid density, pipeline diameter, flow velocity, and friction factor. The friction factor depends on the Reynolds number, which depends on the fluid kinematic viscosity, and the ratio of pipeline roughness to diameter. The pressure drop is directly proportional to the friction factor and fluid density. For the same velocity and diameter, the Reynolds number is higher for LH_2 than for LNG, as LH_2 has a lower kinematic viscosity than LNG ($1.92 \bullet 10^{-7}$ vs $3.19 \bullet 10^{-7}$ m^2/s), resulting in a lower friction factor. LH_2 also has a lower density than LNG (70 vs 470 kg/m^3). A maximum liquid velocity of around 4 m/s is typically adopted in the LNG industry [28]. Therefore, velocities higher than 4 m/s are expected for LH_2, which entails smaller pipeline diameters. Vacuum-insulated pipelines (VIPs) are commonly employed to minimize heat transfer to cryogenic fluids. VIP consists of two concentric pipes: the inner pipe carries the LH_2, while the outer pipe provides structural support, and the annular space is evacuated to reduce or eliminate conductive and convective heat transfer. Additionally, materials such as multi-layer insulation (MLI) or perlite could be used in the annular space to reduce radiative heat transfer. The thermal conductivities across the insulation of these materials range between 0.006 and 0.0008 W/(m•K) [30]. Linde and PHPK Technologies report an overall heat transfer coefficient of 0.026 W/(m^2•K) for VIP incorporating MLI, which is ten times lower than foam insulation [31]. Jord's MLI vacuum pipeline features a 45 mm radial vacuum gap and a heat leak value of approximately 3 W/m^2 [32]. It is equipped with an internal expansion joint (bellows), that allows the core pipe to self-compensate for thermal contractions [32]. Vacuum-insulated pipelines are generally delivered pre-tested and sealed with a life-long vacuum, leaving only the end-to-end interfaces to be welded and the joints to be spot-insulated.

The typical loading rate for large-scale LNG facilities ranges between 10000 and 12000 m^3/h [28]. To facilitate the start and end of the loading operation, ramp-up and ramp-down of the flow rate is a general practice, and each requires approximately 1 h [33]. A typical loading arm for LNG service features a 16-inch (0.4 m) nominal diameter with a capacity of roughly 5000 m^3/h. Depending on the system's hydraulic requirements, two or three loading arms are often used. An additional arm is dedicated to handling boil-off gas generated on the ship during loading, which is then returned to the onshore export terminal. Similar arrangements are anticipated for large-scale LH_2 loading systems. In some instances, when the storage tank is warm, the cooling of the ship's tanks must proceed gradually to minimize thermal stresses. The rate at which a cargo tank can safely be cooled depends on the design of its containment system [34]. It is essential to consult the ship's operating manual to determine the permissible cool-down rate, considering factors such as temperature uniformity, which varies due to cargo tank size and the positioning of spray nozzles. In the LNG industry, this cool-down operation is often supervised directly by the tank vendor.

2.4. LH_2 carrier

Kawasaki Heavy Industries' carrier Suiso Frontier is the first and so-far the only example of a working vessel for LH_2 transportation. It is equipped with a 1250 m^3 type-C tank and has been operational since 2021 between Australia and Japan [35]. In 2022, KHI announced that it had obtained approval in principle from Nippon Kaiji Kyokai (ClassNK) to build a large-scale LH_2 carrier, featuring four type-B tanks with a total capacity of 160000 m^3 [36]. The BOG from these tanks will be used as fuel to power the ship. In 2023, McDermott's unit CB&I received approval in principle from DNV for its design of a liquid hydrogen carrier. CB&I developed this system in collaboration with Shell. The design is based on CB&I's vacuum-insulated spherical technology for onshore LH_2 storage. The company anticipates the design will be scalable to 40000 m^3 per tank, with estimated boil-off rates of less than 0.1 % per day [37].

Type-B tanks are prismatic or spherical vessels that are built independently from the ship and offer low design pressure (<0.7 barg). They are designed to withstand the dynamic loads encountered during marine transportation. No pressure build-up is allowed during transport; hence the design often includes the use of BOG to fuel the ship's engine. Type-B tanks are usually found in large-scale liquefied gas carriers, while type-C tanks (pressure vessels, typically rated for pressures in the range of 7–10 bar) are commonly used for smaller volumes and applications permitting higher-pressure containment, such as in trucks or small ships.

3. System description

The LH_2 export terminal considered in this study is designed for liquefied hydrogen storage, carrier loading and BOG recycling. The system is designed to represent a realistic, short-term implementable case. The locations of the import and export terminals are selected based on the availability of existing infrastructure for LH_2 or, if absent, for LNG. The size of the equipment components—such as storage tanks (both onshore and on-board the ship), pipelines, and pumps—is chosen according to commercially available models or existing prototypes. The terminal is assumed to be located in Karratha (Western Australia, Australia) and supplied by a nearby liquefaction plant, having a base production capacity of 450 t/d LH_2. Karratha is chosen for its advantageous location for exporting to Asia and its established role as a liquefied natural gas export hub. The selection of export terminal location mainly impacts the economics but not BOG generation. The liquefaction plant is assumed to be at a 200 m distance from the export terminal. A LH_2 carrier, based on the design by Kawasaki Heavy Industries (KHI), with four spherical tanks providing a total volume of 160000 m^3 [36], is used to deliver the liquefied hydrogen to Osaka (Japan). Four onshore storage tanks, each with a capacity of 50000 m^3, have been selected based on the proposed larger-scale LH_2 export between Victoria and Japan. Fig. 1 presents a simplified schematic of the entire LH_2 export terminal.

Liquid hydrogen from the liquefaction plant is stored onshore while awaiting the ship's arrival. After filling the storage tanks (which can take many days), LH_2 is then loaded (using LH_2 submerged pumps) from the onshore tanks to LH_2 ship tanks through two 500-m-long pipelines. BOG generated from ship's tanks is compressed slightly and sent to the onshore storage tanks via another pipeline, where it is combined with onshore BOG and sent back to the liquefaction plant using a second compressor. The terminal is subdivided into the following subsystems.

- Onshore Storage System, consisting of four vacuum-insulated spherical-shape LH_2 storage tanks, each with a volume of 50000 m^3, resulting in a combined storage capacity of 200000 m^3;
- Offshore Storage System (LH_2 carrier), with four Moss-type spherical tanks, each with a volume of 40000 m^3, resulting in a total capacity of 160000 m^3;
- Loading System, comprising submerged LH_2 pumps, valves and two LH_2 loading lines, each with a 24-inch (0.6 m) diameter and 500 m in length;
- BOG Return System, consisting of compressors, one 24-inch (0.6 m) diameter, 500-m-long BOG return pipeline from the LH_2 carrier to the LH_2 onshore storage area, and one 8-inch (0.2 m) diameter, 200-m-long BOG return pipeline to the liquefaction plant.

Table 1
Main design parameters of the LH_2 export terminal.

Subsystem	Characteristics and Design Parameters
Onshore Storage System	Storage capacity: 200000 m^3 (4 × 50000 m^3); tank shape: sphere (diameter = 45.7 m); inner tank construction material: stainless steel; outer tank construction material: carbon steel; insulation: glass bubbles under vacuum; minimum operating pressure: 1.013 bar; maximum operating pressure: 1.15 bar; design operating pressure: 1.075 bar.
Offshore Storage System	Storage capacity: 160000 m^3 (4 × 40000 m^3); tank shape: sphere (diameter = 42.4 m); inner tank construction material: stainless steel; outer tank construction material: carbon steel; insulation: glass bubbles under vacuum; minimum operating pressure: 1.013 bar; maximum operating pressure: 1.15 bar; design operating pressure: 1.075 bar.
Loading System	Pump capacity: 8040 m^3/h (4 × 500 m^3/h and 1 × 10 m^3/h for each storage tank); number of loading pipelines: 2; pipeline nominal diameter: 24 inches; pipeline Schedule: 5S; pipeline length: 500 m; inner pipe construction material: stainless steel; outer pipe construction material: carbon steel; insulation: vacuum multi-layer insulation.
BOG Return System	Onshore compressor capacity: 7600 m^3/h (2300 m^3/h + 5300 m^3/h); offshore compressor capacity: 11,500 m^3/h; onshore pipeline nominal diameter: 8 inches; onshore pipeline Schedule: 5S; onshore pipeline length: 200 m; offshore pipeline nominal diameter: 24 inches; offshore pipeline Schedule: 5S; offshore pipeline length: 500 m; inner pipe construction material: stainless steel; outer pipe construction material: carbon steel; insulation: vacuum multi-layer insulation.

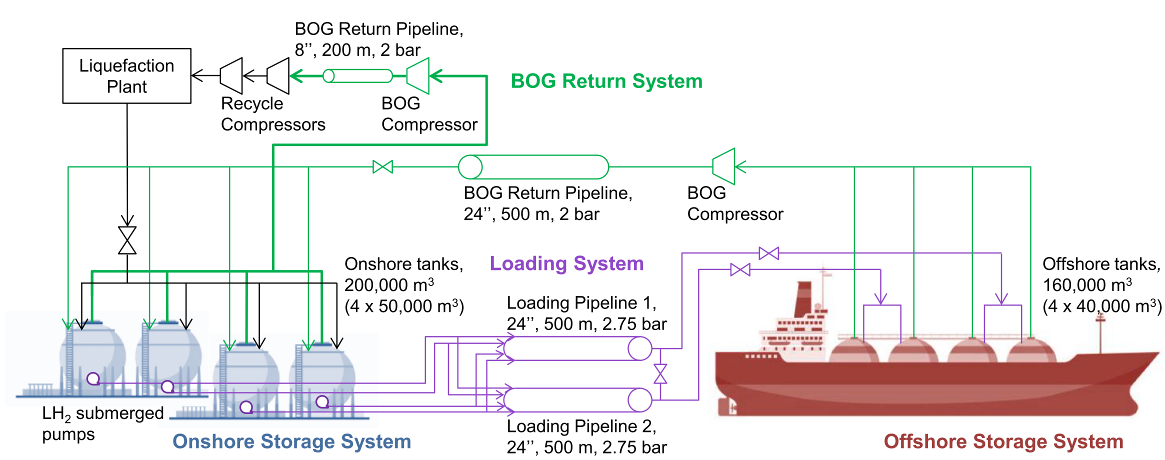

Fig. 1. LH_2 export terminal, where the following subsystems are highlighted: Onshore Storage System (blue), Offshore Storage System (red), Loading System (violet), BOG Return System (green).

Table 1 summarises the main design parameters of the LH_2 export terminal. The total onshore storage capacity is designed to be 25 % greater than the carrier capacity. The tanks' operating pressure is maintained at 1.075 bar, with a maximum pressure of 1.15 bar and a minimum pressure of 1.013 bar (same as ambient pressure), similar to the current LNG practice (note that the pressure unit bar represents the absolute pressure in this work). The maximum flow rate during loading operations is assumed to be 8000 m^3/h. Following LNG practice, a maximum liquid hydrogen velocity of 4 m/s in pipelines is considered, even though higher flow rates are feasible, corresponding to a 0.6 m pipeline diameter. Each onshore tank is equipped with four LH_2 pumps, each with a capacity of 500 m^3/h, to manage the loading flow rate, and one pump with a capacity of 10 m^3/h, to handle the lower flow rate required for circulation while waiting for the ship's arrival at the port. A capacity of 500 m^3/h for each pump is selected to mimic the current maximum flow rate as described by Cryostar [29]. At the beginning and end of the loading operation, the ramp-up and ramp-down of the flow rate are performed in increments of 2000 m^3/h every 15 min to complete the operation within 1 h, similar to the current LNG practice. This is done by adding in or cutting out one pump per onshore tank at each step.

4. Dynamic simulation of LH_2 onshore storage and ship loading

Due to the time-dependent nature of the boil-off gas generation during LH_2 storage and carrier loading operations, a dynamic simulation is necessary for its investigation.

The simulation of a dynamic process is based on solving a set of differential and algebraic equations that describe the time-dependent behaviour of the system. These equations are derived from conservation principles (mass, energy, and momentum balances), along with thermodynamic and empirical correlations for physical properties and kinetics.

- Mass and component balances

$$\frac{d(\rho_{out}\cdot V)}{dt} = \dot{V}_{in}\rho_{in} - \dot{V}_{out}\rho_{out}$$
$$\frac{d(c_{out,j}\cdot V)}{dt} = \dot{V}_{in}\cdot c_{in,j} - \dot{V}_{out}\cdot c_{out,j} + r_j\cdot V \tag{1}$$

where.

$\dot{V}_{in}$ and $\dot{V}_{out}$ are the inlet and outlet volumetric flow rates, respectively
ρ_{in} and ρ_{out} are the inlet and outlet mass density, respectively
V is the volume of the system
t is the time
c_{in} and c_{out} are the inlet and outlet molar concentration, respectively
r is the rate of generation due to chemical reaction
subscript j refers to the j-th component

These differential equations are written for each phase. The total mass balance and component balances are not independent. For a system containing NC components, in general, the total mass balance and NC-1 component balances are typically considered.

- Energy balance

$$\frac{d[e\cdot\rho_{out}\cdot V]}{dt} = \dot{V}_{in}\cdot\rho_{in}\cdot e_{in} - \dot{V}_{out}\cdot\rho_{out}\cdot e_{out} + \dot{Q} + \dot{Q}_r - (\dot{W} + \dot{V}_{out}\cdot P_{out} - \dot{V}_{in}\cdot P_{in})$$
$$e = u + k + \phi \tag{2}$$

where.

e is the total energy per unit mass
u is the internal energy per unit mass
k is the kinetic energy per unit mass
ϕ is the potential energy per unit mass
$\dot{Q}$ is the heat added across system boundaries per unit time
$\dot{Q}_r$ is the heat generated by reaction per unit time
$\dot{W}$ is the shaft work done by the system per unit time
P_{in} and P_{out} are the pressures of the inlet and outlet streams, respectively

- Momentum balance

Navier-Stokes equations express the system momentum balance. However, in practice, empirical hydraulic correlations—such as valve equations, frictional pressure loss relationships in pipes, and pump or compressor performance curves—are typically used to describe the pressure-flow behaviour.

- Phase equilibrium and thermodynamics phase equilibrium (equality of fugacity for each component in the vapour and liquid phases) and physical properties are calculated through algebraic equations
- Reaction kinetics if chemical reactions are present, rate expressions must be considered.
- Controller and equipment models control loops and equipment dynamics (e.g., valves, compressors, heat exchangers) are represented by empirical transfer functions or simplified first-order differential equations.

The material end energy balance equations are written as Ordinary Differential Equations (ODE), assuming negligible thermal and concentration gradients within the control volume (i.e., the system is perfectly mixed and spatially uniform).

In this work, the process, described in Section 3, is modelled using Aspen HYSYS® V12.1 [38] software. The set of differential-algebraic equations is numerically solved within the simulation software using the Implicit Euler method with an integration time step of 0.1 s.

The MBWR (Modified Benedict-Webb-Rubin) thermodynamic package is selected to compute hydrogen properties. MBWR is used because, as noted by Rezaie Azizabadi et al. [39], the MBWR package accurately predicts the thermodynamic properties of hydrogen and parahydrogen across the temperature and pressure ranges relevant to hydrogen liquefaction processes. It outperforms other packages available in the Aspen HYSYS environment, including Peng-Robinson (PR), Soave-Redlich-Kwong (SRK), and Benedict-Webb-Rubin-Starling (BWRS). For example, regarding the mass density predictions of hydrogen (20 K–300 K, 1 MPa), the relative deviations compared to the experimental data reported by Leachman et al. [40] and REFPROP [41] predictions are as follows: (0.24–8.33) % for PR; (−2.00 to 0.12) % for MBWR, (−77.22 to 41.47) % for BWRS and (−0.25 to 8.08)% for SRK. A screenshot of the Aspen HYSYS® simulation flowsheet for the LH_2 export terminal is provided in Section S1 of the Supplementary Material. The simulation models pure para-hydrogen, assuming that the conversion from normal-hydrogen to para-hydrogen is completed during liquefaction. The base ambient temperature is set to 298.15 K. The Process Flow Diagram (PFD) of the plant is shown in Fig. 2. The inlet stream (LH_2) has a mass flow rate $F_{LH2} = 450$ t/d (controlled by FCV-100 and FIC-100), pressure $P_{LH2} = 4$ bar, and vapour fraction $\alpha_{LH2} = 0$ (saturated condition). The discharge of the onshore BOG compressors is set to 2 bar. In the following Section 4.1, the investigated scenarios are defined. Subsequently, Section 4.2 provides details on equipment design and modelling within Aspen HYSYS®, and Section 4.3 presents the method adopted for the economic assessment.

4.1. Scenario definition

Two scenarios are investigated in this work: start-up (Section 4.1.1),

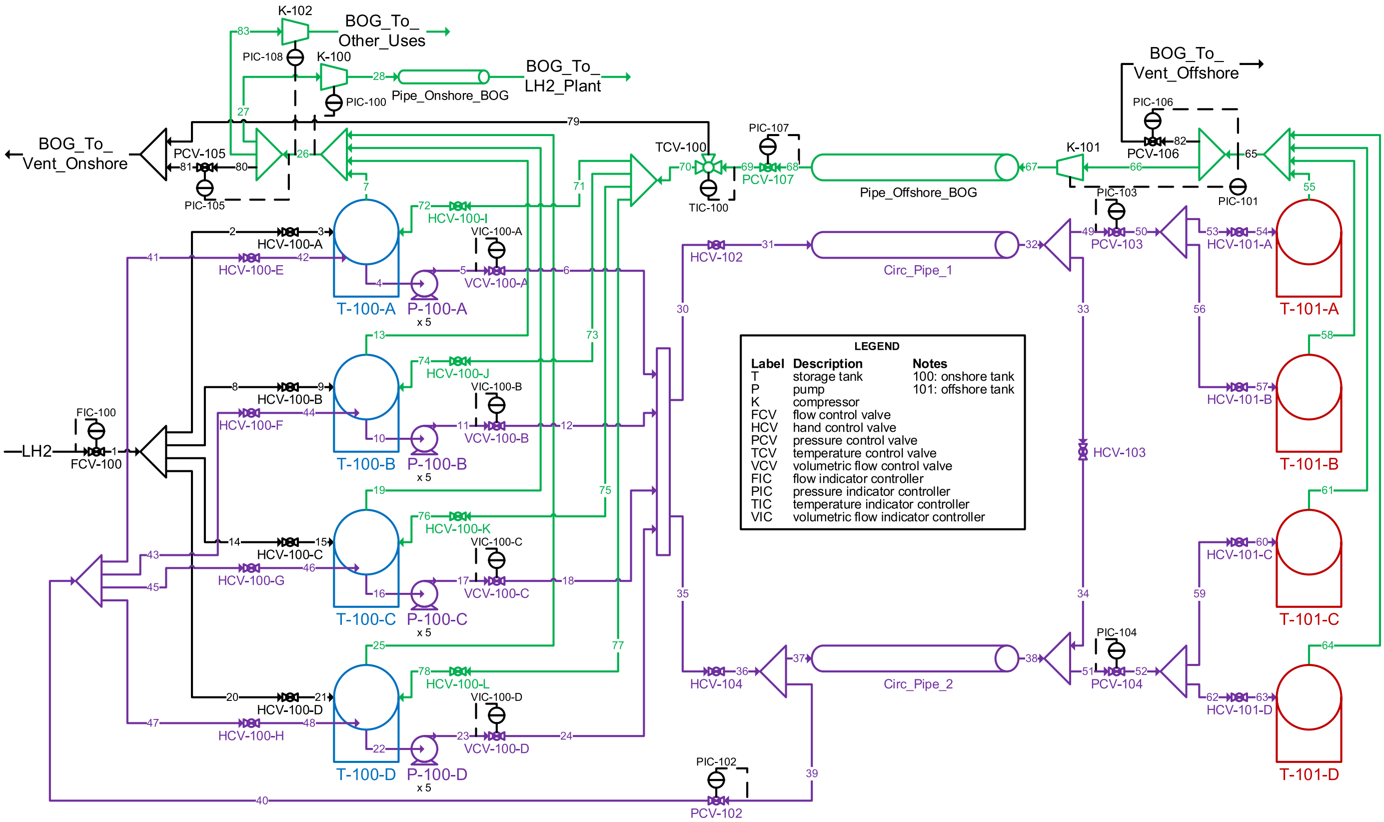

Fig. 2. PFD of the LH_2 export terminal, where the following subsystems are highlighted: Onshore Storage System (blue), Offshore Storage System (red), Loading System (violet), BOG Return System (green).

expected to be a rare occurrence during the plant's lifetime, and normal operation (Section 4.1.2), which represents the typical cyclic way in which the plant operates.

4.1.1. Start-up

At the beginning of the plant's operation, all equipment must undergo a drying and inerting process. This involves purging the equipment with an inert gas such as nitrogen to remove moisture and air, as the presence of oxygen poses a risk of fire or explosion. Since nitrogen freezes at LH_2 temperatures, it must be purged with hydrogen gas before LH_2 is introduced. The present analysis begins at the end of these preliminary operations, with the storage tanks and piping being filled with pure gaseous para-hydrogen at ambient conditions ($T = 298.15$ K, $P = 1.013$ bar). The start-up of the plant includes the following subsequent modes.

- Holding mode
  - Warm holding mode (I): Onshore storage tanks start at ambient temperature. The onshore storage tanks are cooled to 20 K, and then filled until their liquid volume percentage reaches 10 %.
  - Cold holding mode (II): Onshore storage tanks are at LH_2 temperature (20 K), while loading lines start at ambient temperature. Onshore storage tanks are then filled with LH_2 until their liquid volume percentage reaches 90 % or other set value. Meanwhile, LH_2 from the storage tanks is circulated through the loading lines to keep them cold. The initial liquid volume percentage of 10 % ensures a proper head for the pumps used to cool down the loading lines.
- Loading mode
  - Warm loading mode (III): Offshore storage tanks start at ambient temperature. LH_2 is pumped at an initially low flow rate from the onshore storage tanks via the loading lines to the offshore storage tanks. The tanks are cooled until liquid hydrogen starts to accumulate there.
  - Cold loading mode (IV): Offshore storage tanks and loading lines are at LH_2 temperature. LH_2 from the onshore tanks is pumped at a high flow rate into the offshore storage tanks until their liquid volume percentage reaches 98 % or another set value.

4.1.2. Normal operation

The warm holding mode (I) and the early stage of cold holding mode (II) (cooling of the loading line and filling of the onshore storage tank to a certain liquid volume percentage) are likely one-off operations for a real storage and loading system, as the onshore storage tank will, most likely, be kept partially liquid-filled and cold after the first filling until a plant shutdown. The same applies to the warm loading mode (III) and the early stage of cold loading mode (IV) since it is common practice for LNG to retain some cargo (heel) after unloading. Therefore, the normal operation includes normal holding mode (II^+) and normal loading mode (IV^+), defined as follows.

- Holding mode
  - Normal holding mode (II^+): Onshore storage tanks are at LH_2 temperature and partially filled with LH_2. Meanwhile, the loading lines are at LH_2 temperature and filled with circulating LH_2 from onshore storage tanks. Onshore storage tanks are being filled by rundown from the liquefaction plant until their liquid volume percentage reaches 90 % or a set value.
- Loading mode
  - Normal loading mode (IV^+): Offshore storage tanks are at LH_2 temperature and partially filled with LH_2. LH_2 from the onshore tanks is pumped (high flow rate) to fill the offshore storage tanks until their liquid volume percentage reaches 98 % or a set value. Loading lines are already cold.

The results of the start-up scenario, detailed in Section 5.1, indicate that the fill in the onshore storage tanks drops to about 15 % of capacity after loading mode and, hence, this fill level is taken as the starting point for the normal holding mode (II^+). The initial liquid volume in the offshore storage tanks is set to 5 % of capacity, following LNG industry recommendations.

4.2. Equipment design

4.2.1. Onshore and offshore storage tanks

Both the onshore (T-100-A/B/C/D in Fig. 2) and offshore (T-101-A/B/C/D in Fig. 2) storage tanks have a spherical shape. Each onshore tank has a volume of 50000 m^3, while each offshore tank has a volume of 40000 m^3. A detailed heat transfer model is specified, which takes into account natural convection inside and outside the vessel and conduction in the wall and insulation layers. The properties of the inner metal (stainless steel) layer and outer insulation (vacuum glass bubble technology) layer are detailed in Table 2.

The overall heat transfer coefficient, which depends on the temperature profile, is updated during integration. The choice of insulation material (and thus thermal conductivity) greatly impacts the BOG rate. Perlite vacuum insulation has a thermal conductivity ranging from 0.0009 to 0.003 W/(m•K), depending on the vacuum pressure (0.1–10 Pa). Other promising alternatives include the glass microspheres or bubbles used by NASA, which have a thermal conductivity of 0.0007–0.0017 W/(m•K), also depending on the vacuum pressure (0.1–10 Pa) [23]. However, achieving a high vacuum inside the annulus is a time-consuming process. For example, NASA took 42 days to evacuate a 200 m^3 annulus to 100 millitorr (13 Pa) [42].

4.2.2. Submerged pumps

In Fig. 2, P-100-A/B/C/D represent the combined pump sets installed in each onshore tank. Each set consists of four pumps with a capacity of 500 m^3/h each and one pump with a capacity of 10 m^3/h. An overall pump efficiency, being the product of isentropic (80 %) and electrical/mechanical efficiencies (94 %), of 75 % is assumed. The pumps provide a pressure increase of 2 bar to ensure a proper driving force during carrier loading. Since they are of the submerged type, the heat generated during pumping is directly transferred to the surrounding liquid, resulting in an outlet temperature equal to that of the liquid stored in the tanks. To simulate this, a dummy heat exchanger (not shown in Fig. 2) is placed downstream of each pump set and is specified with a zero pressure drop and an outlet temperature matching the temperature of the corresponding vessel (T-100-A/B/C/D in Fig. 2). The heat duty removed by this dummy heat exchanger is supplied to T-100-A/B/C/D.

4.2.3. Circulation/loading pipelines and BOG transport pipelines

The pipelines Circ_Pipe_1, Circ_Pipe_2 and Pipe_Offshore_BOG (see Fig. 2), which connect the onshore and offshore storage tanks, are 500 m long. The pipeline Pipe_Onshore_BOG (see Fig. 2), connecting the onshore tanks to the liquefaction plant, is 200 m long. In the solution algorithm, the pipeline is subdivided into several sub-volumes where the temperature, compositions and reaction rate, are constant through each sub-volume, varying only with time. The accuracy of the numerical solution depends on the number of increments into which the pipeline length is divided. Following a sensitivity analysis, 50 increments are used for the 500-m pipelines, and 20 increments for the 200-m pipeline. The diameter of each pipeline is determined in order to meet the proposed velocity of 4 m/s for liquid service and 20 m/s for vapour service. Consequently, Circ_Pipe_1, Circ_Pipe_2 and Pipe_Offshore_BOG have a 24-inch diameter, with an inner diameter (ID) of 0.5985 m and an outer diameter (OD) of 0.6096 m, based on the industrial standard for stainless steel pipelines with a 5S schedule. Pipe_Onshore_BOG has a 8-inch diameter with ID of 0.21354 m and OD of 0.21908 m. The properties of the inner metal (stainless steel) layer and insulation layer (vacuum multi-layer technology) are reported in Table 3. The overall heat transfer coefficient is updated during integration.

Pressure drop calculations utilize the Beggs and Brill correlation [43]. The pipeline roughness is set according to Aspen HYSYS® [38] recommendations for mild steel ($4.572 \cdot 10^{-5}$ m).

4.2.4. Compressors

In Fig. 2, K-100, K-101 and K-102 are BOG compressors that operate at an extremely low suction temperature, approximately 21 K. Given the current uncertainties on the performances of such compressors, an isentropic efficiency of 50 % is assumed. K-100, with a maximum capacity of 2300 m^3/h, controls the pressure of the onshore tanks during filling. Suction pressure is controlled by adjusting the compressor's rotational speed. Similarly, K-101, which has a capacity of 11500 m^3/h, manages the pressure of the offshore tanks. K-102, with a maximum capacity of 5300 m^3/h, is turned off during holding (onshore tanks' filling) and operates only during carrier loading to handle the increased BOG generated from filling these tanks. The discharge pressure is set to 2 bar, hence, the BOG compressors provide a pressure increase of about 0.85–0.95 bar, depending on suction conditions.

4.2.5. Control loops

The feed flow rate is controlled by FIC-100, which adjusts the actuator position of valve FCV-100. The set point (SP) is 450 t/d, but at the beginning of the start-up scenario, during the first cooling of the onshore storage tanks, the SP is initially set to 150 t/d for the first 24 h and then increased to 300 t/d for the subsequent 24 h. Gradually increasing the flow rate during cooling helps prevent excessive BOG generation and pressure build-up in the tanks.

The onshore tank pressure is regulated by a compressor (K-100) and a valve (PCV-105). The compressor speed is adjusted by the controller PIC-100 to maintain the pressure of the onshore tank header at the SP value of 1.075 bar. The safety valve is normally closed and opens when the tank pressure exceeds the maximum operating pressure of 1.15 bar. This condition is likely to occur during the initial cooling of the tanks or when an unexpected change in process conditions causes high BOG generation. Similarly, the offshore tanks have a common header, whose pressure is controlled by compressor K-101 and valve PCV-106.

The volumetric flow rate circulated in the pipelines to keep them cold while waiting for the ship to be loaded (holding mode) is controlled by VCV-100-A/B/C/D and set to 10 m^3/h. A simple case study investigating different circulation rates suggests that BOG is reduced with lower LH_2 circulation through the pipelines. While this may seem obvious, it is important to recognize that reducing the flow rate changes the temperature profile within the loading lines. Consequently, when switching from holding to loading mode, this increased pipeline temperature will cause boil-off of the loading fluid. This adversely affects both BOG and time management during the loading operation. Therefore, the circulation flow rate is set to maintain a single-phase liquid

Table 2
Properties of the storage tanks material layers.

Property	Metal layer	Insulation layer
Thickness s [m]	0.018	1.403
Specific heat capacity c_p [kJ/(kg•K)]	0.51	0.75
Mass density ρ [kg/m^3]	7930	460
Thermal conductivity k [W/(m•K)]	150	0.0007

Table 3
Properties of the pipeline material layers.

Property	Metal layer	Insulation layer
Thickness s [m]	(OD–ID)/2	0.050
Specific heat capacity c_p [kJ/(kg•K)]	0.51	0.82
Mass density ρ [kg/m^3]	7930	520
Thermal conductivity k [W/(m•K)]	150	0.001

state with a temperature at or below the saturated temperature at loading conditions for the stream at the outlet of the loading lines. This ensures that no additional BOG will be generated during loading, as the pipe temperature will match the LH_2 loading temperature.

During the cooling of offshore tanks, the loading rate is typically governed by the cooldown time of the ship tank material. However, the offshore tank pressure control is found to be a more critical condition for selecting the volumetric flow rate during cooldown operation. A flow rate of 10 m^3/h is set for the first 48 h to ensure that the offshore storage tank pressure does not exceed the maximum operating pressure of 1.15 bar. After this period, the flow rate is increased to 50 m^3/h for the remainder of the cooling operation. This achieves a cooling rate of approximately 5 K/h, which is significantly lower than what is recommended by LNG practices.

Once the offshore storage tanks are cooled, loading begins. The normal loading rate is 8000 m^3/h (2000 m^3/h from each onshore tank). To achieve this rate, the flow is ramped up in steps of 2000 m^3/h (500 m^3/h from each tank) every 15 min. When the liquid volume in the offshore tanks reaches 96 %, the flow rate is gradually reduced using the same steps. After 1 h, the ramp-down is complete, and the liquid volume in the offshore tanks is approximately 98 %. The pressure inside the LH_2 pipelines is maintained at 2.75 bar during both holding and loading modes. This is controlled by pressure control valve PCV-102 during holding, and by PCV-103/104 during loading. In holding mode, PCV-103/104 and HCV-104 are closed, allowing LH_2 to flow from the onshore tanks into Circ_Pipe_1, then into Circ_Pipe_2, and finally back to the onshore tanks, as shown in Fig. 3. In loading mode, PCV-102 and HCV-103 are closed, while HCV-104 and PCV-103/104 are open, allowing LH_2 to flow from the onshore tanks, through Circ_Pipe_1 and Circ_Pipe_2 in parallel to the offshore tanks (see Fig. 3).

The valve PCV-108 controls the pressure inside the pipeline Pipe_Offshore_BOG to 2 bar. The three-way valve TCV-100, controlled by TIC-100, directs the BOG generated offshore to the onshore storage tanks when its temperature is below 60 K, and to the vent when the temperature is above 60 K. This arrangement prevents excessive vaporisation by avoiding the introduction of warm vapour into the onshore tanks. The process control design data are given in Section S2 of the Supplementary Material.

4.3. Method for the economic assessment

A Class 4 costing, or feasibility study [44], of the proposed export terminal is conducted. The Levelized Cost Of Hydrogen (*LCOH*) is calculated according to Eq. (2):

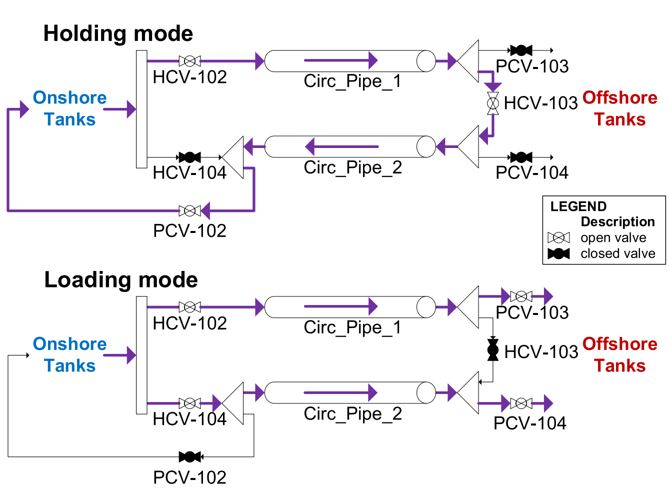

Fig. 3. Flow direction within pipelines during holding and loading modes.

$$LCOH = \frac{\sum_{t=0}^{t_p-1} \frac{CAPEX(t)+OPEX(t)}{(1+I_{fix})^t}}{\sum_{t=0}^{t_p-1} \frac{F_{delivered}(t)}{(1+I_{fix})^t}} \tag{3}$$

where $F_{delivered}$ is the mass flow rate, in kg/y, of hydrogen delivered to Japan, t is the year, with 0 being the base year and t_p being the plant lifetime, *CAPEX(t)* and *OPEX(t)* are the capital and operating expenditures, in USD/y, at time t and I_{fix} is the fixed annual interest (discount) rate. The assumptions for the economic assessment are detailed in Table 4.

The duration of the ship's supply cycle (ship loading, trip from Australia to Japan, ship unloading and trip from Japan to Australia) is calculated as the sum of.

- the round-trip transit time, based on a one-way sea distance of about 7400 km and an average speed of 16 knots (approximately 30 km/h);
- the time needed for loading and unloading operations, computed by doubling the sum of the normal loading times (assuming that the ship unloading takes the same time as its loading), derived from simulation results, and the ship preparation time, assumed to be 12 h;
- a safety margin of 2 days to handle potential delays [46].

The shipping cycle duration must be compared with the overall time needed for normal operation of the loading process to determine the number of ships required under continuous production. The amount of LH_2 delivered, $F_{delivered}$, is calculated considering that the ship utilizes gaseous hydrogen as fuel and that the heel is 5 %. Gaseous hydrogen is obtained either by warming the boil-off gas generated during sea transport or, if insufficient, by evaporating the required amount from the LH_2 cargo and then warming it. The boil-off gas rate during shipping is assumed to be equal to 0.2 %/d [46]. Due to the lack of data on LH_2 carriers' propulsion engines, the fuel consumption rate is estimated based on the LNG consumption rate of a LNG carrier with similar capacity [47], considering that hydrogen has approximately 2.5 times the heating value of natural gas on a mass basis and assuming identical engine efficiency. Based on these assumptions, the fuel consumption rate is estimated at 40 t/d.

The investment cost method implemented in this work is based on equipment purchase cost functions and percentage cost factors to account for delivery and installation [48]. The cost-capacity functions that are used to estimate equipment purchase cost C_p are given in Table 5; these functions are adapted from literature, and updated to the year 2023 using the Chemical Engineering Plant Cost Index (CEPCI). Spare units for pumps and compressors are considered. An equipment installation factor ($f_{ins,eq}$) is then used to estimate the total equipment cost (bare module cost). The equipment installation factor depends on the equipment type and complexity and varies largely from one piece of equipment to another. This is adapted from literature and considers everything that is needed to install and commission a particular equipment such as labour costs, foundations, structures, insulation, piping, electrical and instrumentation.

The cost function for estimating the bare module cost of the pipelines, in USD, is taken from the literature [55] and adapted to the base year using the CEPCI. The resulting equation is:

Table 4
– Assumptions for the economic assessment.

Item	Value
Base year ($t = 0$)	2023
Fixed annual interest rate I_{fix}	8 %
Plant lifetime t_p	25 y
Plant availability	95 %
Construction period	3 y (*CAPEX* subdivision: 40 %, 30 %, 30 %)
Decommissioning cost	5 % *CAPEX* [45]

Table 5
Purchase cost of equipment functions.

Equipment	Characteristic size A	C_p [USD]	Ref. C_p	$f_{ins,eq}$	Ref. $f_{ins,eq}$
Storage tank	Gross volume [m^3]	$C_p = 7.354 \cdot 10^4 \cdot A^{0.6210}$	[49–52]	1.3	[49]
Carrier	Gross volume [m^3]	$C_p = 7.635 \cdot 10^5 \cdot A^{0.5136}$	[47,53,54]	1.3	assumption
Pump	Volumetric flow rate [m^3/h]	$C_p = 1.739 \cdot 10^4 \cdot A^{0.4237}$	[49,50]	1.3	[49]
Compressor	Power [kW]	$C_p = 1.584 \cdot 10^5 \cdot A^{0.4240}$	[49–51]	2	[49]

$$C_{\mathrm{BM,pipeline}} = \left(1.032 \cdot A_1^2 + 13.44 \cdot A_1 + 290.5\right) \cdot A_2 + 6.803 \cdot 10^5 \tag{4}$$

where A_1 is the nominal diameter of the pipeline, in inches, and A_2 is the pipeline length, in m. An additional general installation factor, f_{ins}, is considered, which accounts for the cost contributions of engineering and supervision, construction, overhead and administration, site preparation, offsite capital, general electrical and safety systems, contracting fee, project execution, and commissioning. This factor is often reported as a multiplier of the total equipment cost [56], and for this study, a value of $f_{\mathrm{ins}} = 1.6$ is adopted based on the recent work of Lee et al. [57]. Additionally, a location factor ($f_{\mathrm{loc}} = 1.2$ [58]) is considered when estimating the total *CAPEX*. The *OPEX* for utility consumption are related to the electricity consumption of pumps and compressors, which is retrieved from the simulation. The price of electricity is estimated to be 0.093 USD/kWh, based on the wholesale price for Western Australia [59]. Operating and maintenance costs are calculated as a fixed percentage of the annual *CAPEX*, and assumed to be 10 % [46].

5. Results and discussion

In this Section, process simulation results are presented for the two scenarios investigated: start-up (Section 5.1) and normal operation (Section 5.2). For normal operation, which represents the plant's usual functioning after the initial start-up, a BOG recovery strategy is discussed (Section 5.2.1). A techno-economic assessment is also performed to quantify the hydrogen export cost (Section 5.2.2). Then, in Section 5.2.3, a sensitivity analysis is carried out to assess the impact of feed flow rate, LH_2 feed pressure and ortho-para hydrogen composition on the operation of the export terminal. All these parameters depend upon the design of the liquefaction plant that serves the terminal.

5.1. Start-up scenario

The results in terms of duration and total BOG in each mode of operation and for the overall process are reported in Table 6. The start-up scenario lasts 39.3 days, with cold holding mode accounting for about 75 % of the total time. A total of 401.5 tonnes of BOG are generated, primarily during the warm holding and warm loading modes. Overall, BOG generation represents about 19 % of the LH_2 feed for the process as a whole. Storage tank cool-down from ambient temperature to 20 K takes 2.3 days, which is similar to current LNG practice; this considers the time taken to cool down the inner vessel and insulation fully. Depending on the scenario and the total amount of BOG generated, three options are considered for the BOG recovery: recycling BOG to the nearby liquefier, venting or flaring BOG (in extreme cases) and utilising BOG for other applications. This will be discussed further in Section 5.2.1. Venting (or flaring) BOG is only considered for the warm holding mode (I) and warm loading mode (III) during the start-up scenario, which occurs only once during the plant start-up process.

Detailed simulation strip charts are shown in Figs. 4 and 5. Fig. 4 represents the temperature (top) and filling fraction (bottom) for the onshore and offshore storage tanks. Looking at this figure, it is possible to identify the different modes according to their definition. During warm holding mode (I), the temperature of the onshore tanks decreases from ambient temperature to the hydrogen saturation temperature at 1.075 bar, with the rate steepening as the flow rate increases. During the filling of the onshore tanks (the last part of warm holding mode and the entire cold holding mode (II)), the temperature of the onshore tanks remains constant while their liquid volume percentage gradually increases over time. The temperature of the offshore tanks remains constant and equal to the ambient temperature during holding mode (I + II) and decreases to the liquid hydrogen temperature during warm loading mode (III). During cold loading mode (IV), the temperature of the offshore tanks remains constant while their liquid volume percentage increases. Simultaneously, the liquid volume percentage in the onshore tanks decreases as their content is transferred to the offshore tanks. Fig. 5 represents the tank pressures (at the top) and BOG mass flow rates (at the bottom) as functions of time. It is possible to notice that during

Table 6
Key results of start-up scenario at each operation mode and the overall process.

Mode	Duration (days)	Total BOG To Vent (t)	Total BOG To LH_2 Plant (t)	Total BOG To Other Uses (t)	Overall BOG Percentage of F_{LH2} (%)
Warm holding (I)- Tank cool-down	2.3	179.2	51.8	82.3	30.7
Warm holding (I)- Tank filling to 10 %	3.7	0.0	286.6	0.0	17.1
Cold holding (II)	29.5	0.0	2193.6	0.0	16.5
Warm loading (III)	2.9	222.1	158.4	0.0	29.1
Cold loading (IV)	0.9	0.1	64.0	132.1	50.8
Overall (I + II + III + IV)	39.3	401.5	2754.4	214.5	19.1

Total BOG To Vent: integral over time of the BOG flow rate from the onshore and offshore vents.

Total BOG To Vent $= \int_{t_{\mathrm{mode,i}}}^{t_{\mathrm{mode,i+1}}} \left(F_{\mathrm{BOG\ To\ Vent\ Onshore}} + F_{\mathrm{BOG\ To\ Vent\ Offshore}}\right) dt$

Total BOG To LH_2 Plant: integral over time of the BOG flow rate to the liquefaction plant.

Total BOG To LH_2 Plant $= \int_{t_{\mathrm{mode,i}}}^{t_{\mathrm{mode,i+1}}} \left(F_{\mathrm{BOG\ To\ LH2\ Plant}}\right) dt$

Total BOG To Other Uses: integral over time of the BOG flow rate to other uses.

Total BOG To Other Uses $= \int_{t_{\mathrm{mode,i}}}^{t_{\mathrm{mode,i+1}}} \left(F_{\mathrm{BOG\ To\ Other\ Uses}}\right) dt$

Overall BOG Percentage of F_{LH2}: sum of all the BOG contributions, divided by the duration and by the feed flow rate.

Total Overall BOG = Total BOG To LH2 Plant + Total BOG To Other Uses + Total BOG To Vent

Overall BOG Percentage of $F_{\mathrm{LH2}} = \dfrac{\text{Total Overall BOG}}{\text{Duration} \cdot F_{\mathrm{LH2}}}$

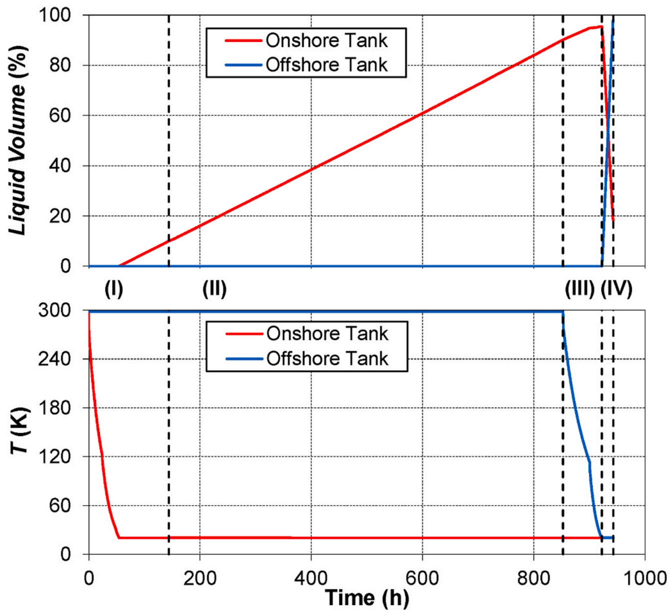

Fig. 4. Onshore and offshore storage tanks' liquid volume percentage (top) and temperature, *T*, (bottom) as a function of time. Each section between the vertical dashed lines represents a different operation mode: (I) Warm holding mode; (II) Cold holding mode; (III) Warm loading mode; (IV) Cold loading mode.

the tanks' cool-down, warm holding mode (I), and warm loading mode (III), the amount of BOG generated is extreme, leading to tank pressure rising to the maximum operating pressure. At this point, the safety relief valves open, venting some of the BOG generated to maintain tank pressure within operating ranges. As previously mentioned, this is only a one-time operation, and thus, venting some BOG is considered reasonable given that during this one-time operation, the amount of BOG generated cannot be handled by the compressors used to control the pressure inside the storage tanks. Furthermore, during warm loading mode (III), the BOG from the offshore tanks is generated at a higher temperature. If this warm BOG is fed directly to the onshore tanks, a large amount of vaporisation will occur inside the tank due to the contact with the warm BOG; suggesting the need to vent this one-time BOG generated.

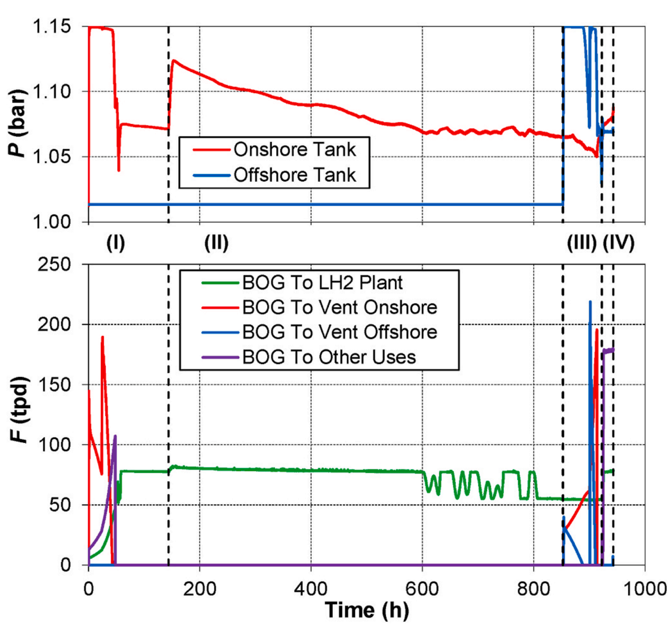

Fig. 5. Onshore and offshore storage tanks' pressure, *P*, (top) and BOG streams' mass flow rate, *F*, (bottom) as a function of time. Each section between the vertical dashed lines represents a different operation mode: (I) Warm holding mode; (II) Cold holding mode; (III) Warm loading mode; (IV) Cold loading mode.

During cold holding mode (II), the generated BOG is almost steady (does not fluctuate much) and can be managed by the onshore BOG compressor K-100. Towards the end of this mode, the dynamic simulation shows that the BOG flow rate fluctuates slightly due to adjustments in compressor speed necessary to maintain tank pressure within the operating ranges. BOG generated during the cold loading mode (IV) is much higher than the cold holding mode (II) due to the high loading rate used to transfer LH_2. In this case both onshore BOG compressors, K-100 and K-102, operate at their maximum capacity to manage the large BOG flows from the onshore tanks. In fact, the sizing of compressor K-102 considers the amount of BOG generated during cold loading mode (IV).

5.2. *Normal operation scenario*

Table 7 reports the results in terms of duration and total amount of BOG for each mode and the overall process. Not having to cool down the storage tanks and loading lines reduced the duration of the normal holding mode (II^+) to 27.5 days, which is 2.01 days and 8.01 days shorter than the start-up cold holding mode (II) and the start-up holding mode (I + II), respectively. Similarly, not having to cool down the offshore storage tanks reduced the duration of normal loading mode (IV^+) to 0.8 days, which is 2.1 days shorter than the loading mode (III + IV) associated with the start-up scenario. Note that during normal operation scenarios, there is no BOG vented; all BOG generated is sent back to the liquefier or utilized for other applications (more details in Section 5.2.1). Throughout the entire normal operation scenario, the overall BOG generation is 17 % of the total LH_2 produced.

Fig. 6 shows the simulation strip charts for the normal operation scenario, in terms of tanks' pressure (at the top) and BOG streams' mass flow rate (at the bottom). It can be observed that during normal holding mode (II^+), the generated BOG is handled solely by the onshore compressor K-100. However, during normal loading mode (IV^+), both onshore BOG compressors, K-100 and K-102, are necessary to manage the BOG generation inside the onshore tanks.

5.2.1. *BOG management and recovery*

Venting or flaring the hydrogen BOG would be the simplest way to dispose of it, but it results in a significant energy loss, especially for a gas that is expensive to produce and liquefy. To avoid wasting BOG, the most viable solution is to reliquefy it by harnessing the nearby liquefaction plant. However, since the liquefaction plant operates steadily, it is necessary to regulate the hydrogen feed by adjusting the electrolysers if green hydrogen is being fed or using buffer tanks to even out the BOG flow rate after compression. This largely depends on the operation mode. For example, during normal holding mode (II^+) operation, the rate of BOG generation fluctuates between 55.3 and 78.9 t/d, as shown in Fig. 5. To maintain the hydrogen inlet to the liquefier at 450 t/d, a variation in the hydrogen flow rate produced by the electrolysers within the range (−4.7 to 1.5) % would be necessary. Alternatively, a fixed amount of BOG sent to the liquefier could be managed. However, this will require buffer tanks to accommodate variable BOG inlet flow rates and a constant outlet flow rate connected to the nearby liquefier. This will result in fluctuating accumulated mass and variable pressure in the buffer tanks. The volume calculations for these buffer tanks are given in Section S3 of the Supplementary Material. Fig. 6 shows the profile of the BOG flow rate managed by compressor K-100 (solid green line), which is intended for reliquefaction at the nearby plant. The average BOG flow rate, represented as a green dashed line in Fig. 6, is 73.1 t/d. When the actual BOG flow rate is greater than the average, the pressure in the buffer tanks rises due to the increase in accumulated mass. Conversely, when the flow rate is lower than the average, the pressure decreases.

Table 7
Key results of normal operation scenario at each operation mode and the overall process.

Mode	Duration (days)	Total BOG To LH_2 Plant (t)	Total BOG To Other Uses (t)	Overall BOG Percentage of F_{LH2} (%)	Average *F* BOG To LH_2 Plant (t/d)
Normal holding (II^+)	27.5	2007.7	0.0	16.2	73.0
Normal loading (IV^+)	0.8	65.2	147.0	57.3	79.3
Overall (II^++IV^+)	28.3	2072.9	147.0	17.4	73.1

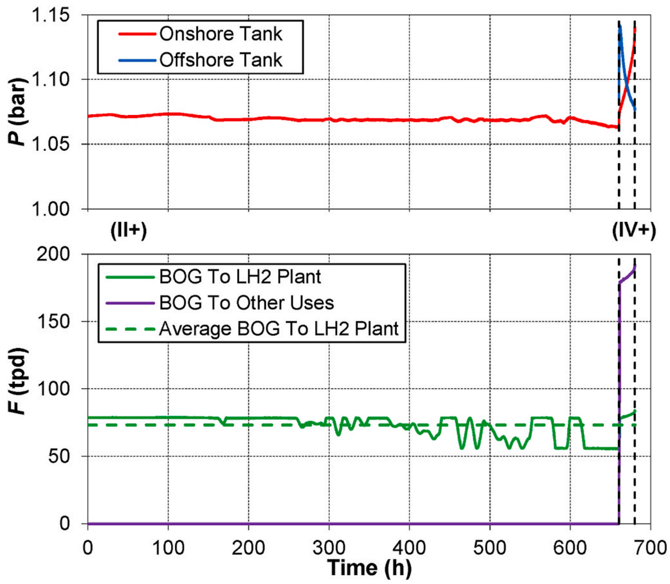

Fig. 6. Onshore and offshore storage tanks' pressure, *P*, (top) and BOG streams' mass flow rate, *F*, (bottom) as a function of time. Each section between the vertical dashed lines represents a different operation mode: (II^+) Normal holding mode; (IV^+) Normal loading mode.

Because of the low density of hydrogen at ambient temperature and moderate pressures, the buffer tanks are expected to have a large volume. Assuming a pressure variation between 30 and 40 bar within the buffer tanks, the volume required to supply vapour BOG to the liquefier at a constant flow rate of 73.1 t/d would be approximately 100000 m^3. This volume requirement would result in significant capital expenditure, making it a financially unfeasible solution. The buffer tank pressure profile and the buffer tank inlet and outlet mass flow rates as a function of time during the normal holding operation are shown in Section S3 of the Supplementary Material.

In some instances, such as during cold loading modes, some of the generated BOG might need to be sent for other uses due to the excessive amount of BOG generated during loading operation. For example, during normal loading mode, a second onshore compressor, K-102, is used to manage the excess BOG flow rate, which K-100 cannot handle (see the violet line in Fig. 6). Since this compressor is expected to be used only for a short time (less than 1 day) during each operational cycle, the BOG is envisaged to be compressed and stored at high pressure in appropriate cylindrical vessels. This stored gas can then either be sold as compressed gas or serve as a buffer for the liquefaction process.

Other options for BOG recovery include the use of a dedicated small reliquefaction plant which can handle all BOG generated during normal operation mode. The advantage of this approach is that cryogenic refrigeration can be performed without the need to precool the hydrogen gas, as it is already at a low temperature. However, a control strategy must be implemented in the reliquefaction plant to manage the unsteady supply. Emerging technologies include the use of magnetocaloric materials to reliquefy BOG. Magnetocaloric materials can achieve refrigeration through the magnetocaloric effect, which involves heating and cooling materials by applying and removing a magnetic field. This approach offers the potential for highly efficient and compact cooling systems, reducing the energy consumption associated with traditional cryogenic refrigeration methods but is mainly suitable for small-scale capacity [60]. Additionally, other advanced technologies, such as metal-organic frameworks (MOFs) and adsorption-based systems, are being explored for BOG storage. These technologies are promising, as they generally exhibit high hydrogen uptake at low temperatures and moderate pressures [61].

Table 8
Results of the techno-economic assessment on the considered LH_2 export terminal.

Cost item	Value
$C_{BM,i}$ [M USD]	
Storage Tanks	316.7
Carrier	467.3
Pumps	6.9
Compressors	19.6
Pipelines	4.6
$C_{BM,total}$ [M USD]	815.1
***CAPEX* [M USD]**	1565.0
$OPEX_{utilities}$ [M USD/y]	0.1
$OPEX_{O\&M}$ [M USD/y]	156.5
***OPEX* [M USD/y]**	156.6
***LCOH* [USD/kg]**	2.77

5.2.2. Economic assessment

The shipment time from Karratha to Osaka is calculated to be 25.5 days, while the normal operation of the export terminal takes 28.3 days. Therefore, under the current assumption for the case study, liquefaction capacity of 450 t/d and carrier size of 160000 m^3, approximately 12 shipments are performed in a year, requiring the purchase of only one ship. Cost calculations are summarized in Table 8.

The *CAPEX* for the considered export terminal amounts to 1565.0 M USD, primarily due to the costs for the onshore storage tanks and ship. The *OPEX* is estimated at 156.6 M USD/y, with the electricity consumption of loading pumps and BOG compressors contributing negligibly because the primary driver of *OPEX* is operating and maintenance. The resulting *LCOH* for terminal storage and shipment is 2.77 USD/kg. When this cost is added to the cost of hydrogen production and liquefaction, it becomes clear that cost reduction throughout the entire hydrogen supply chain is necessary to make LH_2 a viable energy carrier. Ishimoto et al. [62] reported a *CAPEX* of 1068 M EUR_{2015} (1657 M USD_{2023}) for a loading terminal comprising three 50000 m^3 storage tanks, and a *CAPEX* of 275 M EUR_{2015} (427 M USD_{2023}) for a LH_2 carrier with a capacity of 86000 m^3. The estimated *LCOH* for the loading terminal and seaborne transport ranges from 1.08 to 2.46 EUR_{2015}/kg, depending on the delivery distance, which varies between 2500 and 23400 km. A *LCOH* of 1.3 EUR_{2020}/kg is reported by Roland Berger [63] for a case study involving sea transport distance of 12000 km and a feed flow rate of 200 t/d, without specifying the equipment size. IEA [64] estimated a *LCOH* of about 1.6 USD_{2017}/kg for the combined export/import terminals and seaborne transport from Australia to Japan. This estimate considers a 160000 m^3 ship with a *CAPEX* of 412 M USD_{2017} (579 M USD_{2023}) and storage tanks with a capacity of 46000 m^3 each, having a *CAPEX* of 290 M USD_{2017} (408 M USD_{2023}). Considering the increase in inflation over the past few years, the *LCOH* estimated in this study aligns with previous projections.

Table 9
Key results of the sensitivity analysis on feed flow rate.

F_{LH2} (t/d)	450	900	1800	450	900	1800	450	900	1800
Mode	Duration (days)			Average F BOG To LH_2 Plant (t/d)			Overall BOG Percentage of F_{LH2} (%)		
Normal holding (II^+)	27.5	13.8	6.9	73.0	149.6	301.4	16.2	16.6	16.7
Normal loading (IV^+)	0.8	0.8	0.8	79.3	154.1	304.6	57.3	36.5	26.8
Overall (II^++IV^+)	28.3	14.6	7.7	73.1	149.9	301.8	17.4	17.7	17.8

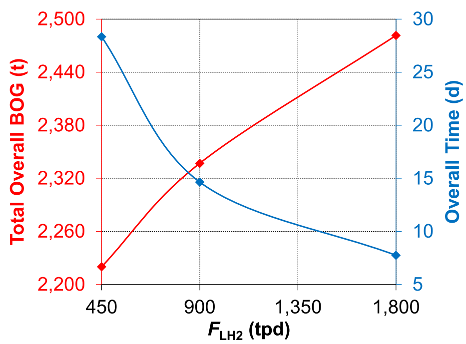

Fig. 7. Results of the sensitivity analysis on feed flow rate: total overall BOG generated (red line) and overall normal operation time (blue line).

5.2.3. Sensitivity analyses

The flow rate of the fed LH_2 to the export terminal is doubled and quadrupled to study the variation in shipping frequency (duration of holding mode) and overall BOG generation. The results are detailed in Table 9. Fig. 7 illustrates the trends of total overall BOG generated and overall normal operation time as functions of the feed flow rate.

The overall cycle time for the export terminal in normal operations decreases from 28.3 to 14.6 days when the feed flow rate is doubled, and to 7.7 days when it is quadrupled. A shipping frequency similar to LNG is achieved when the LH_2 feed rate is 1800 t/d. However, the capacity of existing hydrogen liquefaction plants is far below this value (current maximum capacity is around 32 t/d). Substantial research and investment are necessary to scale operations to this level. Only the normal holding time is affected by the feed flow rate, as the loading time is governed by the maximum capacity of the pumps (thus total loading rate), resulting in a non-linear relationship between overall time and feed flow rate, as shown in Fig. 7. The overall BOG percentage of the LH_2 feed remains almost constant but slightly increases with the feed flow rate due to faster vapour displacement. However, the total overall BOG generated increases less than proportionally, as shown in Fig. 7, due to the reduced holding time and, consequently, lower BOG generated from total heat ingress from the environment and total heat dissipated by the pumps during this holding mode.

Shipping frequency could also be reduced by considering a smaller onshore and offshore storage capacity. When the storage capacity is reduced by half, the overall cycle time for the export terminal in normal operations decreases from 28.3 to 14.4 days, as shown in Table 10. However, the overall BOG percentage of the LH_2 feed increases from 17.4 % to 18.8 %. This is because the heat ingress from the ambient per unit storage volume rises due to the higher surface-to-volume ratio of the tanks. The average BOG flow rate to the liquefaction plant increases slightly for the same reason.

The pressure of the LH_2 feed is varied in the range 2–6 bar to study its impact on the performance of the export terminal. This pressure corresponds to the operating pressure of the last flash separator in the liquefaction plant. A higher feed pressure increases the saturation temperature, thereby reducing the cooling duty required for liquefaction. However, a higher feed pressure to the export terminal increases BOG generation due to larger pressure depressurization (flash evaporation). This study assesses quantitatively the effect of pressure on the performance of the export terminal, as shown in Table 11. Nevertheless, the optimal pressure level should be selected considering the combined performance of the liquefaction, storage, and export facilities. Fig. 8 shows how the overall BOG generation and the feed temperature $T_{sat,LH2}$ (saturation temperature at the specified pressure) vary with feed pressure.

The total overall BOG generated increases linearly with the feed pressure (red line in Fig. 8), indicating that flashing due to depressurization represents a substantial contribution to BOG generation at the export terminal. However, since the vapour pressure has an exponential relationship with temperature, a given pressure difference corresponds to a larger temperature difference at lower pressures (see the blue line in Fig. 8). Therefore, a moderate pressure appears to be the best trade-off between the total amount of BOG generated, with the consequent energy requirements for its recovery, and the temperature of the LH_2 fed to the export terminal, which impacts the energy consumption of the liquefaction plant. The power consumption of a liquefaction process can be represented by the Specific Energy Consumption (SEC, kWh/kg_{LH2}), a function of the net power consumption (kW) and the LH_2 product mass flowrate (kg/h). For a traditional refrigeration cycle, the net power consumption is the difference between the total power consumption and total power recovered (by the turbine expanders). In this case, elevating the LH_2 feed or BOG pressure can reduce compressor power by lowering the required compression ratio, thereby decreasing the specific work input per unit mass. However, the increased storage pressure also leads to a substantial rise in BOG generation, which increases the total mass flow to be compressed. As a result, the overall compression power may increase despite the lower specific compression requirement, highlighting a trade-off between pressure-driven efficiency gains and BOG quantity-induced energy penalties.

The sensitivity analysis on the ortho-para hydrogen composition of the feed stream is investigated to understand the effects of a potential catalyst malfunction in the liquefaction plant on BOG generation during storage at the export terminal. When the catalyst works properly, the ortho-para hydrogen composition at the end of the liquefaction process is close to equilibrium. at about 99.6 % para-hydrogen. However, if the

Table 10
Key results of the sensitivity analysis on storage capacity.

Offshore storage capacity (m^3)	160,000	80,000	160,000	80,000	160,000	80,000
Onshore storage capacity (m^3)	200,000	100,000	200,000	100,000	200,000	100,000
Mode	Duration (days)		Average F BOG To LH_2 Plant (t/d)		Overall BOG Percentage of F_{LH2} (%)	
Normal holding (II^+)	27.5	13.9	73.0	78.1	16.2	17.3
Normal loading (IV^+)	0.8	0.4	79.3	80.0	57.3	70.0
Overall (II^++IV^+)	28.3	14.4	73.1	78.1	17.4	18.9

Table 11
Key results of the sensitivity analysis on feed pressure.

P_{LH2} (bar)	2	4	6	2	4	6	2	4	6
Mode	Duration (days)			Average F BOG To LH_2 Plant (t/d)			Overall BOG Percentage of F_{LH2} (%)		
Normal holding (II^+)	24.9	27.5	30.4	32.4	73.0	108.9	7.2	16.2	24.2
Normal loading (IV^+)	0.8	0.8	0.8	32.1	79.3	116.2	40.4	57.3	64.9
Overall (II^++IV^+)	25.7	28.3	31.2	32.4	73.1	109.1	8.3	17.4	25.3

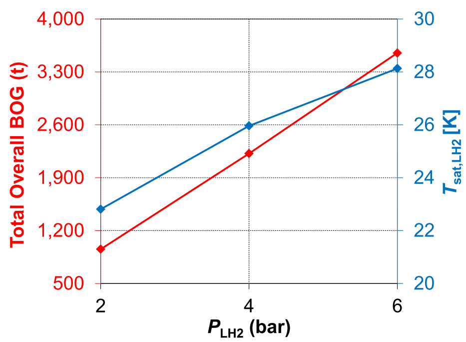

Fig. 8. Results of the sensitivity analysis on feed pressure: total overall BOG generated (red line) and feed saturation temperature (blue line).

catalyst loses effectiveness due to poisoning or degradation, the resulting liquid hydrogen will have a non-equilibrium composition, leading to slow ortho-para conversion during storage, which ultimately produces additional BOG due to the exothermic nature of the ortho-to-para conversion. The natural (non-catalysed) ortho-para conversion follows a second-order reaction rate:

$$\frac{dc}{dt} = -kc^2 + k'c(1-c) \tag{5}$$

where c is the ortho-hydrogen molar concentration, k and k' are the rate constants for the forward (ortho-to-para) and reverse (para-to-ortho) reactions, respectively. Milenko et al. [65] measured k and k' for liquid and gaseous hydrogen from 16.65 K to 120 K, at pressures up to 70 MPa and proposed correlations depending on temperature, mass density and ortho-hydrogen molar fraction at equilibrium. In this work, the pressure and temperature conditions inside the tanks are almost constant and equal to 1.075 bar (operating design pressure) and 20.47 K (saturation temperature at the design pressure), hence the values of k and k' are calculated with the correlation proposed in Ref. [65] at these conditions and kept constant.

The sensitivity analysis involved varying the feed para-hydrogen molar fraction $x_{para\text{-}H2,LH2}$, from 25 % (normal-hydrogen composition) to 99.59 % (equilibrium composition at 20.47 K). Fig. 9a shows the results in terms of liquid filling and hold-up composition of the onshore tanks after 27.5 days (normal holding time in the base case). The trends of total overall BOG generated and hold-up composition of the offshore tanks at the end of normal operation are illustrated in Fig. 9b.

Fig. 9a shows that feeding LH_2 with a composition different from equilibrium results in a lower liquid volume percentage inside the onshore tanks after a fixed period, which is the normal holding time in the base case (see the red line in Fig. 9a). This decrease is so significant that, when filling the onshore storage tanks with normal-hydrogen instead of equilibrium-hydrogen, the liquid volume percentage will be 27 % instead of 90 % after the same period. If normal hydrogen continues to be fed, it will take 385 days for the onshore tanks to reach 90 % capacity. Since the natural ortho-para conversion is a slow reaction, there is insufficient time for the contents of the onshore tanks to reach equilibrium if a non-equilibrium hydrogen mixture is fed. The para-hydrogen percentage in the tanks decreases with that of the feed according to the blue line in Fig. 9a. The results depicted in Fig. 9b are obtained by stopping the simulation after 28.3 days (normal operation time in the base case) or earlier if the liquid volume percentage in the onshore tanks drops below 10 %. It can be observed that below 90 % para-H_2 content in the feed, the total overall BOG generated increases linearly with the decrease in feed para-H_2 content (red line in Fig. 9b). The extent of this increase is more than 1000 t for every 10 percentage points, indicating that the feed hydrogen composition greatly affects BOG generation.

6. Conclusions

This work is a case study based on the operation of a postulated LH_2 export terminal and offers insights into the key factors that affect operation and boil-off gas generation. For the base case examined, involving a liquid hydrogen feed flow rate of 450 t/d and a carrier size of 160000 m^3, the normal operation cycle of the plant is about 28 days, during which all the BOG generated can be recovered. This is achieved by recovering an almost constant flow rate throughout the operational cycle and managing the higher BOG generated during carrier loading with dedicated equipment with low annual operational time. However, during the start-up, BOG losses through the vents are unavoidable while cooling the tanks to maintain the tank's pressure below the maximum design threshold. Therefore, keeping the tanks partially filled during

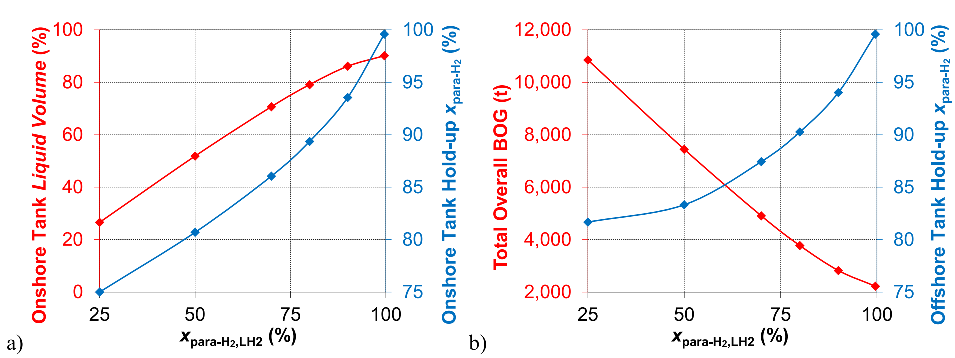

Fig. 9. Results of the sensitivity analysis on feed ortho-para hydrogen composition: a) onshore tank liquid volume percentage (red line) and onshore tank hold-up para-H_2 percentage (blue line) at the end of normal holding mode (after 27.5 days); b) total overall BOG generated (red line) and offshore tank hold-up para-H_2 percentage (blue line) at the end of normal loading mode (28.3 days or until onshore tank liquid volume percentage drops below 10 %).

normal operation is essential to avoiding any BOG. This study also highlights the importance of ensuring pressure profiles within the tanks remain within safe operating limits, which has a high impact on the loading and unloading operations. The levelized cost of hydrogen for terminal storage and shipment is estimated at 2.77 USD/kg, highlighting the need for further research to reduce costs before liquid hydrogen export can be considered economically viable. The sensitivity analysis carried out reveals that increasing the feed flow rate is beneficial for both increasing shipping frequency, reducing the normal operation time to about 8 days when the flow rate is 1800 t/d (4 times the base rate), and comparatively decreasing the percentage of overall boil-off gas generation. LH_2 feed pressure to the export terminal significantly impacts BOG generation during holding, as flashing due to depressurization is a primary contributor to BOG generation in the onshore storage tanks. The total overall BOG generated increases threefold when the feed pressure is raised from 2 to 6 bar. Achieving ortho-para hydrogen equilibrium composition at the end of the liquefaction process is found to be crucial since a deviation from equilibrium would cause a significant increase in BOG. When the para-H_2 content in the feed is below 90 %, the total BOG generated increases linearly with the decrease in para-H_2 content, exceeding 1000 tons for every 10 % decrease in para-H_2 content, surpassing the capacity of the BOG compressors designed for normal operation mode.

This study represents a first step towards evaluating the viability of utilising liquefied hydrogen to transport low-cost Australian hydrogen to Japan. The viability of this supply chain depends not only on liquefaction efficiency but also critically on the effective management and minimisation of BOG losses during storage, loading, and unloading operations. This analysis demonstrates that BOG losses during transfer can be substantial, underscoring the urgent need for targeted mitigation strategies. To achieve commercial scalability, future efforts should provide detailed comparison of various recovery strategies that accounts for economic and technical feasibility and focus on developing and integrating efficient BOG recovery systems, tailored to specific operational modes and customer requirements. For instance, when the liquefier is located near the export terminal, recycling BOG back to the liquefier (during normal operation)—as explored in this study—is a highly recommended approach. The findings presented here provide a quantitative foundation to guide future system design and policy development, while clearly outlining research pathways aimed at reducing BOG losses and improving the overall performance of liquid hydrogen supply chains.

CRediT authorship contribution statement

Federica Restelli: Writing – original draft, Visualization, Validation, Software, Methodology, Investigation, Formal analysis. **Fuyu Jiao:** Writing – original draft, Visualization, Software, Methodology, Investigation, Formal analysis, Conceptualization. **Bruce Norris:** Supervision. **J.P. Martin Trusler:** Writing – review & editing, Supervision, Methodology. **Arman Siahvashi:** Investigation. **Eric F. May:** Writing – review & editing, Supervision, Resources, Project administration, Methodology. **Laura A. Pellegrini:** Writing – review & editing, Supervision, Methodology. **Michael Johns:** Writing – review & editing, Supervision, Resources, Project administration, Methodology. **Saif Z.S. Al Ghafri:** Writing – original draft, Supervision, Resources, Methodology, Formal analysis, Data curation, Conceptualization.

Declaration of competing interest

The authors declare that they have no known competing financial interests or personal relationships that could have appeared to influence the work reported in this paper.

Acknowledgements

The work has been supported by the Future Energy Exports CRC (www.fenex.org.au) whose activities are funded by the Australian Government's Cooperative Research Centre Program. This is a FEnEx CRC Document 2025/23.RP2.0161-FNX-MILE0889.

Appendix A. Supplementary data

Supplementary data to this article can be found online at https://doi.org/10.1016/j.energy.2025.139715.

Data availability

Data will be made available on request.

References

[1] IEA. Global hydrogen review 2022. Paris, France: IEA; 2022. https://www.iea.org/reports/global-hydrogen-review-2022.
[2] IEA. Global hydrogen review 2023. Paris, France: IEA; 2023. https://www.iea.org/reports/global-hydrogen-review-2023.
[3] DoE US. DOE national clean hydrogen strategy and roadmap. 2022.
[4] Australian Government. Department of climate change energy the environment and water. National Hydrogen Strategy; 2024.
[5] Restelli F, Spatolisano E, Pellegrini LA, de Angelis AR, Cattaneo S, Roccaro E. Detailed techno-economic assessment of ammonia as green H_2 carrier. Int J Hydrogen Energy 2024;52:532–47.
[6] Kim H, Kim A, Byun M, Lim H. Comparative feasibility studies of H_2 supply scenarios for methanol as a carbon-neutral H_2 carrier at various scales and distances. Renew Energy 2021;180:552–9.
[7] Spatolisano E, Restelli F, Matichecchia A, Pellegrini LA, de Angelis AR, Cattaneo S, et al. Assessing opportunities and weaknesses of green hydrogen transport via LOHC through a detailed techno-economic analysis. Int J Hydrogen Energy 2024;52:703–17.
[8] Al Ghafri S, Munro S, Cardella U, Funke T, Notardonato W, Trusler JPM, et al. Hydrogen liquefaction: a review of the fundamental physics, engineering practice and future opportunities. Energy Environ Sci 2022;15:2690–731.
[9] Hydrogen energy supply chain. HESC, https://www.hydrogenenergysupplychain.com/; [accessed 28 May 2024].
[10] LATTICE Technology. LATTICE technology hold collaboration meeting with Northern Territory Government. https://lattice-technology.com/darwins-projects/. [Accessed 28 May 2024].
[11] CSIRO. Darwin Green Liquid Hydrogen (LH2) export Project. https://research.csiro.au/hyresource/darwin-green-liquid-hydrogen-lh2-export-project/. [Accessed 28 May 2024].
[12] CSIRO. Central Queensland Hydrogen (CQ-H2. Project. https://research.csiro.au/hyresource/central-queensland-hydrogen-project/. [Accessed 28 May 2024].
[13] Kim J, Vu HTT, Kim S, Choi M, Lee E, Park K, et al. Technical feasibility of large-scale transportable liquid hydrogen export terminal. Int J Hydrogen Energy 2024;66:499–511.
[14] Morales-Ospino R, Celzard A, Fierro V. Strategies to recover and minimize boil-off losses during liquid hydrogen storage. Renew Sustain Energy Rev 2023;182:113360.
[15] Gursu S, Lordgooei M, Sherif SA, Veziroğlu TN. An optimization study of liquid hydrogen boil-off losses. Int J Hydrogen Energy 1992;17(3):227–36.
[16] Okpeke BE, Ait Aider C, Baetcke L, Ehlers S. Assessment of boil-off losses and their cost implication during liquid hydrogen tank filling with and without precooling. Energies 2024;17(16):4092.
[17] Wang J, Webley PA, Hughes TJ. Thermodynamic modelling of pressurised storage and transportation of liquid hydrogen for maritime export. Int J Hydrogen Energy 2024;62:1273–85.
[18] Smith JR, Gkantonas S, Mastorakos E. Modelling of boil-off and sloshing relevant to future liquid hydrogen carriers. Energies 2022;15(6):2046.
[19] Kim D, Trædal S, Berstad DO, Nekså P, Yum KK. Hydrogen re-liquefaction process for boil-off gas handling on a large-scale liquid hydrogen carrier. Conference hydrogen re-liquefaction process for boil-off gas handling on a large-scale liquid hydrogen carrier. ICCEX Praha.
[20] Choi M, Jung W, Lee S, Joung T, Chang D. Thermal efficiency and economics of a boil-off hydrogen re-liquefaction system considering the energy efficiency design index for liquid hydrogen carriers. Energies 2021;14(15):4566.
[21] Ravichandran K, Cavaliere PD. Seasonal analysis of boil-off gas rates in liquid hydrogen storage tank using time-series analysis. Int J Hydrogen Energy 2025;128:725–31.
[22] Petitpas G. Simulation of boil-off losses during transfer at a LH_2 based hydrogen refueling station. Int J Hydrogen Energy 2018;43(46):21451–63.
[23] Fesmire J, Swanger A, Jacobson J, Notardonato W. Energy efficient large-scale storage of liquid hydrogen. Conference Energy efficient large-scale storage of liquid hydrogen, vol. vol 1240. IOP Publishing, p. 012088.

[24] Inomata A, Hashimoto S, Yamanouchi K, Yamamoto T. Hydrogen storage - development of liquefied hydrogen terminal. Kawasaki Technical Review 2021; 182:29–34.
[25] Heavy Industries Kawasaki. Kawasaki completes basic design for world's largest class (11,200-cubic-meter) spherical liquefied hydrogen storage tank. https://global.kawasaki.com/en/corp/newsroom/news/detail/?f=20201224_8018. [Accessed 28 May 2024].
[26] Samsung C&T. Samsung C&T develops design for world's largest liquefied hydrogen storage tank. https://news.samsungcnt.com/en/features/engineering-construction/2024-02-samsung-ct-develops-design-for-worlds-largest-liquefied-hydrogen-storage-tank/. [Accessed 28 May 2024].
[27] Kim H-K. Samsung C&T to build world's largest liquid hydrogen tank. https://www.kedglobal.com/hydrogen-economy/newsView/ked202311130004. [Accessed 28 May 2024].
[28] Pelto PJ, Baker EG, Holter GM, Powers TB. Overview study of LNG release prevention and control systems. 1982.
[29] Cryostar. Liquid hydrogen transfer pumps. https://cryostar-hydrogen-solutions.com/liquid-hydrogen-transfer-pumps/. [Accessed 28 May 2024].
[30] Śliwa T, Kruszewski M, Zare A, Assadi M, Sapińska-Śliwa A. Potential application of vacuum insulated tubing for deep borehole heat exchangers. Geothermics 2018; 75:58–67.
[31] Linde Engineering & PHPK Technologies. Vacuum insulated piping for LNG service. https://www.phpk.com/wp-content/uploads/2019/09/2008Brochure.pdf. [Accessed 28 May 2024].
[32] Jord. Vacuum Insulated Pipe (VIP). https://www.jord.com.au/expertise/lng-vacuum-insulated-piping/. [Accessed 28 May 2024].
[33] Azalea Maritime. LNG marine loading terminal information. Cargo Handling Agreement, http://www.azalea-maritime.com/LNG_CCR_Resource_Management_Training_Materials/1.4%20Load%20Terminal%20Info%20Cargo%20Handling%20Agreement3.pdf; [accessed 28 May 2024].
[34] McGuire JJ, White B. Liquefied gas handling principles on ships and in terminals. third ed. Great Britain: Witherby & Co Ltd; 2000.
[35] Hydrogen Energy Supply Chain. The suiso frontier. https://www.hydrogenenergysupplychain.com/about-the-pilot/supply-chain/the-suiso-frontier/. [Accessed 24 May 2024].
[36] Kawasaki Heavy Industries. Kawasaki obtains AIP for large, 160,000 m3 Liquefied Hydrogen Carrier, https://global.kawasaki.com/en/corp/newsroom/news/detail/?f=20220422_3378&wovn=it;2022. [accessed 28 May 2024].
[37] McDermott. CB&I receives approval for liquid hydrogen cargo containment system for gas carriers from DNV. https://www.mcdermott-investors.com/news/press-release-details/2023/CBI-Receives-Approval-for-Liquid-Hydrogen-Cargo-Containment-System-for-Gas-Carriers-from-DNV/default.aspx. [Accessed 28 May 2024].
[38] AspenTech. Aspen HYSYS®,Burlington (MA), United States. 2021.
[39] Rezaie Azizabadi H, Ziabasharhagh M, Mafi M. Applicability of the common equations of state for modeling hydrogen liquefaction processes in aspen HYSYS. Gas Process J 2021;9(1):11–28.
[40] Leachman JW, Jacobsen RT, Penoncello SG, Lemmon EW. Fundamental equations of state for parahydrogen, normal hydrogen, and orthohydrogen. J Phys Chem Ref Data 2009;38(3):721–48.
[41] Eric W, Lemmon IHB, Huber Marcia L, McLinden Mark O. Refprop 10.0: NIST standard reference database 23. Refprop 100: NIST Standard Reference Database, vol. 23; 2018.
[42] Sass JP, Cyr WWS, Barrett TM, Baumgartner RG, Lott JW, Fesmire JE. Glass bubbles insulation for liquid hydrogen storage tanks. Conference Glass bubbles insulation for liquid hydrogen storage tanks, vol. 1218. American Institute of Physics, p. 772-779.
[43] Payne GA, Palmer CM, Brill JP, Beggs HD. Evaluation of inclined-pipe, two-phase liquid holdup and pressure-loss correlation using experimental data (includes associated paper 8782). J Petrol Technol 1979;31(9):1198–208.
[44] Bates J, Burton CDJ, Creese RC, Hollmann JK, Humphreys KK, McDonald Jr DF, et al. Cost estimate classification system. AACE, Inc.; 2013.
[45] Lorenczik S, Kim S, Wanner B, Bermudez Menendez JM, Remme U, Hasegawa T, et al. Projected costs of generating electricity. 2020 edition 2020.
[46] Restelli F, Spatolisano E, Pellegrini LA, Cattaneo S, de Angelis AR, Lainati A, et al. Liquefied hydrogen value chain: a detailed techno-economic evaluation for its application in the industrial and mobility sectors. Int J Hydrogen Energy 2024;52: 454–66.
[47] International Gas Union. World LNG report, 27th world gas conference. 2018.
[48] Walas SM. Chemical process equipment: selection and design. 1988.
[49] Nexant Inc, et al. Air liquide, Argonne National Laboratory, Chevron Technology Venture, gas Technology Institute, National Renewable Energy Laboratory. In: H2A hydrogen delivery infrastructure analysis models and conventional pathway options analysis results; 2008.
[50] DOE. Multi-year research, development and demonstration plan - 3.2 hydrogen delivery. 2015.
[51] Wang Y, Kowal J, Leuthold M, Sauer DU. Storage system of renewable energy generated hydrogen for chemical industry. Energy Proc 2012;29:657–67.
[52] Hart D, Howes J, Lehner F, Dodds PE, Hughes N, Fais B, et al. Scenarios for deployment of hydrogen in contributing to meeting carbon budgets and the 2050 target. 2015.
[53] International Gas Union. World LNG Report—2015 Edition, Oslo, Norway. 2015.
[54] Lochner S, Bothe D. The development of natural gas supply costs to Europe, the United States and Japan in a globalizing gas market—Model-based analysis until 2030. Energy Policy 2009;37(4):1518–28.
[55] Parker N. Using natural gas transmission pipeline costs to estimate hydrogen pipeline costs. 2004.
[56] Syed MT, Sherif SA, Veziroglu TN, Sheffield JW. An economic analysis of three hydrogen liquefaction systems. Int J Hydrogen Energy 1998;23(7):565–76.
[57] Lee J-S, Cherif A, Yoon H-J, Seo S-K, Bae J-E, Shin H-J, et al. Large-scale overseas transportation of hydrogen: comparative techno-economic and environmental investigation. Renew Sustain Energy Rev 2022;165:112556.
[58] Humphreys KK. Project and cost engineers' handbook. CRC Press; 2004.
[59] Horizon Power. Electricity fees & charges. https://www.horizonpower.com.au/utilities/pricing/. [Accessed 28 May 2024].
[60] Ihnfeldt R, Feng T, Chen R, Jin S. Technical and economic analysis: small Scale cryogenic magnetic refrigeration systems.
[61] Shet SP, Priya SS, Sudhakar K, Tahir M. A review on current trends in potential use of metal-organic framework for hydrogen storage. Int J Hydrogen Energy 2021;46 (21):11782–803.
[62] Ishimoto Y, Voldsund M, Nekså P, Roussanaly S, Berstad D, Gardarsdottir SO. Large-scale production and transport of hydrogen from Norway to Europe and Japan: value chain analysis and comparison of liquid hydrogen and ammonia as energy carriers. Int J Hydrogen Energy 2020;45(58):32865–83.
[63] Weichenhain U. Hydrogen transportation: the key to unlocking the clean hydrogen economy. 2021.
[64] IEA. The future of hydrogen. Paris, France: IEA; 2019. https://www.iea.org/reports/the-future-of-hydrogen.
[65] Milenko YY, Sibileva RM, Strzhemechny MA. Natural ortho-para conversion rate in liquid and gaseous hydrogen. J Low Temp Phys 1997;107(1):77–92.